Published in final edited form as:
Biochemistry. 2008 December 9; 47(49): 13056–13063. doi:10.1021/bi8015197.

Analysis of the reaction of carbachol with acetylcholinesterase with thioflavin T as a coupled fluorescence reporter†

Terrone L. Rosenberry*, **Leilani K. Sonoda**, **Sarah E. Dekat**, **Bernadette Cusack**, and **Joseph L. Johnson**‡

Mayo Clinic College of Medicine, Departments of Neuroscience and Pharmacology, Jacksonville, Florida, 32224

Abstract

Acetylcholinesterase (AChE) contains a narrow and deep active site gorge with two sites of ligand binding, an acylation site (or A-site) at the base of the gorge and a peripheral site (or P-site) near the gorge entrance. The P-site contributes to catalytic efficiency by transiently binding substrates on their way to the acylation site, where a short-lived acylated enzyme intermediate is produced. Carbamates are very poor substrates that, like other AChE substrates, form an initial enzyme-substrate complex with free AChE (*E*) and proceed to an acylated enzyme intermediate (*E*C) which is then hydrolyzed. However, the hydrolysis of *E*C is slow enough to resolve the acylation and deacylation steps on the catalytic pathway. Here we focus on the reaction of carbachol (carbamoylcholine) with AChE. The kinetics and thermodynamics of this reaction are of special interest because carbachol is an isosteric analog of the physiological substrate acetylcholine. We show that the reaction can be monitored with thioflavin T as a fluorescent reporter group. The fluorescence of thioflavin T is strongly enhanced when it binds to the P-site of AChE, and this fluorescence is partially quenched when a second ligand binds to the A-site to form a ternary complex. Analysis of the fluorescence reaction profiles was challenging, because four thermodynamic parameters and two fluorescence coefficients were fitted from the combined data both for *E* and for *E*C. Respective equilibrium dissociation constants of 6 and 26 mM were obtained for carbachol binding to the A- and P-sites in *E* and of 2 and 32 mM for carbachol binding to the A- and P-sites in *E*C. These constants for the binding of carbachol to the P-site are about an order of magnitude larger (*i.e.*, indicating lower affinity) than previous estimates for the binding of acetylthiocholine to the P-site.

Keywords

Acetylcholinesterase; thioflavin T; carbamoylation; peripheral site; enzyme mechanism

Acetylcholinesterase (AChE)[1] (FOOTNOTE 1) hydrolyzes the neurotransmitter acetylcholine at one of the highest known enzymatic rates (5). Interest in AChE inhibitors has been stimulated

†This work was supported by grant NS-16577 from the National Institutes of Health and by grants from the Muscular Dystrophy Association of America

*Corresponding author: Terrone L. Rosenberry, Ph.D Mayo Clinic 4500 San Pablo Road Jacksonville, FL 32224 e-mail: rosenberry@mayo.edu FAX: (904) 953-7370 Phone: (904) 953-7375

‡Current address: University of Minnesota Duluth, Department of Chemistry and Biochemistry, Duluth, Minnesota 55812

[4]Similar solutions have been derived previously: reference Rosenberry, T. L. (1969), Ph.D. Dissertation, The University of Oregon, Eugene, OR; (3,4).

[1]Abbreviations: AChE, acetylcholinesterase; ATMA, 3-(acetamido)-*N*,*N*,*N*-trimethylanilinium; DTNB, 5,5′-dithiobis-(2-nitrobenzoic acid); M7C, 1-methyl-(7-dimethylcarbamoxy)quinolinium; *Tc*AChE, *Torpedo californica* AChE; TMTFA, *m*-(*N*,*N*,*N*-trimethylammonio)trifluoroacetophenone.

by observations that a number of these inhibitors, including carbamoyl esters, have been shown to have therapeutic benefits. In particular, AChE inhibitors that penetrate the blood-brain barrier elevate the levels of endogenous acetylcholine and are useful in the symptomatic treatment of Alzheimer's disease (6).

A better understanding of the AChE catalytic pathway may identify new mechanisms of AChE inhibition. An essential feature of AChE activity at many cholinergic synapses is the ability to hydrolyze acetylcholine within a millisecond of its release (7). Insights into this high catalytic efficiency were obtained from ligand binding studies (1,8,9) and X-ray crystallography (10, 11), which revealed a narrow active site gorge some 20 Å deep with two separate ligand binding sites. At the base of the gorge is the acylation or A-site where residue W86 [2] (FOOTNOTE 2) binds the trimethylammonium group of acetylcholine and H447, E334, and S203 participate in a triad that catalyzes the transient acylation and deacylation of S203 during each substrate turnover. The peripheral or P-site, spanned by residues W286 near the mouth of the gorge and D74 near a constriction at the boundary between the P-site and the A-site, specifically binds certain ligands like the neurotoxin fasciculin (12,13) and the fluorescent probes propidium (9) and thioflavin T (1).

The translation of these structural insights into a functional understanding of the AChE catalytic mechanism is challenging. A series of previous reports from our laboratory indicates that Scheme 1 provides a minimal mechanistic framework that can account for most catalytic features of AChE (2,4,14-17).

Scheme 1 includes an initial complex with substrate S bound to the P-site (ES$_P$, where the subscript P denotes the ligand bound to the P-site) and a subsequent complex with substrate shifted to the A-site (ES) where S203 is acylated to generate EAP. P in this complex is the initial product that remains after transfer of the acyl group, and the catalytic pathway concludes by dissociation of P and hydrolysis of the acylated enzyme EA to give the second product AOH. Ternary complexes in which intermediates also bind a ligand L at the P-site (ESL$_P$, EAPL$_P$,and EAL$_P$) allow the rate constants for conversion of one intermediate to the next to be altered by the relative factors a, g, or b, respectively. The ligand L may be a second molecule of substrate or an inhibitor with affinity for the P-site. The formation of these ternary complexes can account for substrate hydrolysis profiles that deviate from a classical Michaelis-Menten kinetic formulation. We have reported that substrate inhibition with acetylthiocholine (a decrease in hydrolysis rates v at high S concentration) results from $g \cong 0$ in the EAPS$_P$ complex (15); that substrate activation with the cationic acetanilide ATMA (an increase in v at moderate S concentration) arises from $a \cong > 1$ in the ESS$_P$ complex (2); and that inhibition by P-site inhibitors (I) results in part from low values of k_{S2} in the EI$_P$ complex (14). Others have contended that substrate activation results from $b \cong > 1$ in the EAS$_P$ complex (18). One difficulty in resolving these sometimes conflicting claims is that the rate equation for v that is derived from Scheme 1 has too many unknown kinetic parameters, and a number of very different sets of parameter values fit the data equally well (2,19). Furthermore, some of the reversible reactions in Scheme 1 are not at equilibrium, and in this case v in general can be solved only by numerical integration (2,17). This can add a few more unknown kinetic parameters. Progress can be made, however, by grouping parts of Scheme 1 that are in equilibrium, by choosing substrates that eliminate parts of Scheme 1, and by determining some of the thermodynamic parameters in Scheme 1 by experiments that are independent of measurements of v. All three of these approaches are incorporated in this report.

The class of AChE inhibitors comprised of carbamoyl esters (here referred to as carbamates) are actually very poor substrates for AChE. Like other AChE substrates, they form an initial

[2]Throughout this paper we number amino acid residues according to the human AChE sequence (Uniprot accession number P22303).

enzyme-substrate complex *E*S and proceed to an acylated enzyme intermediate which is then hydrolyzed. However, unlike carboxylic acid ester substrates, the hydrolysis of the carbamoylated enzyme is slow enough to resolve the acylation and deacylation steps. Despite this striking advantage offered by carbamates, few comprehensive analyses of their reactions with AChE have been undertaken. Here we report on the interaction of AChE with carbachol, a carbamate whose reaction mechanism with AChE is particularly important because it is an isosteric analog of acetylcholine (Figure 1). We show that the reaction of carbachol with AChE can be monitored with thioflavin T (Figure 1) as a fluorescent reporter group. The fluorescence of thioflavin T is strongly enhanced when it binds to the P-site of AChE, and this fluorescence is partially quenched when a second ligand binds to the A-site to form a ternary complex (1). These fluorescence changes allow the determination of carbachol affinities for the A- and P-sites both in the free enzyme and in the carbamoylated enzyme intermediate.

Experimental Methods

Materials

Recombinant human AChE was expressed as a secreted, disulfide-linked dimer in *Drosophila* S2 cells and purified as outlined previously (16). Total AChE concentrations (E_{tot}) were calculated assuming 450 units/nmol (1).[3] FOOTNOTE 3. Thioflavin T and carbachol (carbamoylcholine chloride) were from Sigma. Thioflavin T was recrystallized from water, and concentrations were assigned by absorbance at 412 nm with $\varepsilon_{412\ nm}$ = 36,000 $M^{-1}cm^{-1}$ (with water as the solvent).

Fluorescence titration of AChE with thioflavin T

The fluorescence was monitored on a Perkin-Elmer LS-50B luminescence spectrometer thermostatted at 25 °C. Fluorescence excitation was at 450 nm and emission at 490 nm, with excitation and emission slits of 10 to 20 nm. Mixing thioflavin T and AChE in a thermostatted Hi-Tech SFA 20 stopped flow apparatus gave a stable fluorescence signal (F) over a 3 - 4 min recording interval. Average F values were corrected for inner filter effects (20) as described previously (2). Data were consistent with a single thioflavin T binding site on AChE and analyzed with eq 1, a slight extension of a previous equation (1).

$$F=F_B+0.5\left(f_{EL}-f_Q\right)\cdot\left[D-\sqrt{D^2-4[E]_{tot}[L]_{tot}}\right] \quad (1)$$

In eq 1, $D = [E]_{tot} + [L]_{tot} + K_L$, where $[E]_{tot}$ and $[L]_{tot}$ are the total enzyme (*E*) and thioflavin T (L) concentrations, respectively, and K_L is the equilibrium dissociation constant; $F_B = B + f_Q[L]_{tot} + f_E[E]_{tot}$, where B is the blank fluorescence without *E* or L and $f_Q = f_L/(1 + ([L]_{tot}/K_Q))$; and f_L, f_{EL} and f_E are the fluorescence intensity coefficients for free thioflavin T, bound thioflavin T, and free enzyme, respectively. Values of f_L, f_E, B and K_Q were determined from measurements with thioflavin T or enzyme alone. The parameter K_Q was introduced here to account for slight self-quenching at high concentrations of thioflavin T. Data were fitted to eq 1 by unweighted nonlinear regression analysis (Fig.P version 6.0c), with $[L]_{tot}$ as the independent variable and K_L and f_{EL} as the fitted parameters.

[3]One unit of AChE activity corresponds to 1 μmol of acetylthiocholine hydrolyzed/min under standard pH-stat assay conditions at pH 8 (1). Our conventional spectrophotometric assay at 412 nm (2) is conducted in pH 7 buffer. With recombinant human AChE and 0.5 mM acetylthiocholine, this assay results in 4.8 $\Delta A_{412\ nm}$/min with 1 nM AChE or about 76 % of the pH stat assay standard.

Stopped-Flow Measurements of Carbachol Reaction with AChE

Stopped-flow methods were required to accurately measure the approach to the carbamoylation steady state with thioflavin T as a fluorescent reporter ligand. The thermostatted Hi-Tech SFA 20 stopped flow apparatus described above was used to rapidly mix equal volumes (300 ul) of AChE in one syringe and carbachol in the other. Fluorescence measurements were obtained as described above and recorded at fixed intervals as short as 20 msec. Thioflavin T was added at equal concentrations to both syringes in 40 mM sodium phosphate, 0.04% Triton X-100 at pH 7.0. To maintain constant ionic strength when the range of carbachol concentrations extended to 60 mM, additional NaCl was included added so that the sum of the carbachol and NaCl concentrations was 60 mM.

A framework for kinetic analysis of AChE carbamoylation

With carbamate substrates, both the formation and hydrolysis of the acylated enzyme intermediate, or carbamoyl enzyme (*E*C), are slow enough to allow equilibrium assumptions. A general approach is given in Scheme 2 (4,21).

In this scheme, k_{12} is an overall carbamoylation rate constant that incorporates the intrinsic rate constant k_2 from Scheme 1, and k_{21} is an overall decarbamoylation rate constant that incorporates k_3. P and COH are the products released during the carbamoylation and decarbamoylation reactions, respectively. The terms E•M and EC•N represent all species in equilibrium with E and EC, respectively (*i.e.*, [E]•M + [EC]•N = $[E]_{tot}$, where [E] and [EC] are the respective concentrations of E and EC and E_{tot} is the total concentration of enzyme active sites), and M and N are sums of terms (involving rate and equilibrium constants and ligand concentrations) that depend on the details of a selected reaction scheme. The rate equation corresponding to Scheme 2 can be solved explicitly if all ligand concentrations remain essentially constant over the reaction time course (21,22), as recently described (4). When [EC] = 0 at time t = 0, the solutions are given in eqs 2 and 3.

$$[E]\,M=\frac{[E]_{tot}\left(k_{21}+k_{12}\,e^{-[(k_{12}+k_{21})t]}\right)}{(k_{12}+k_{21})} \tag{2}$$

$$[E\mathrm{C}]\;N=\frac{[E]_{tot}\,k_{12}\left(1-e^{-[(k_{12}+k_{21})t]}\right)}{(k_{12}+k_{21})} \tag{3}$$

Determination of carbachol affinities for the AChE A- and P-sites with thioflavin T as a fluorescent reporter

Thioflavin T fluorescence was employed to evaluate the interactions of carbachol at the A- and P-sites during the carbamoylation reaction. In the context of Scheme 2, one expression for the time dependence of F is given by eq 4. In eq. 4, F_0 is the fluorescence at time = 0 and F_F is the fluorescence when carbamoylation has reached a final steady state.

$$F=F_0+(F_F-F_0)\left(1-e^{[(k_{12}+k_{21})t]}\right) \tag{4}$$

F also can be formulated in the more useful terms F_{EM} and F_{ECN}, the respective fluorescence contributions from species equilibrated with E and EC, as shown in eq 5.

$$F=F_B+F_{EM}[E]M+F_{ECN}[EC]N \quad (5)$$

In eq. 5, $F_B = B + f_L[L] + f_S[S]$, where B is the blank fluorescence with *E* in the absence of L or S and the molar fluorescence coefficients f_L and f_S are determined from measurements with thioflavin T or carbachol alone. Combining eqs. 2, 3, and 5 gives eq. 6.

$$F=F_B+F_{EM}[E]_{tot}+\frac{(F_{ECN}-F_{EM})[E]_{tot}k_{12}}{(k_{12}+k_{21})}\left(1-e^{-[(k_{12}+k_{21})t]}\right) \quad (6)$$

While eq 6 provided a good fit to the fluorescence data, we routinely applied a slightly extended version of this equation (eq A2) that permitted incorporation of a slower component of relatively small amplitude (see the Appendix).

Because k_{21} is much smaller than k_{12} for the reaction of virtually all carbamates with AChE, the exponential time course involving conversion of initial *E* to predominant *E*C in the final steady state is readily apparent with thioflavin T as the fluorescent reporter. However, k_{12} and k_{21} are not resolved individually in this fluorescence analysis. Although k_{21} is small, it is not completely negligible relative to k_{12}, and the individual values of these rate constants do slightly influence the fitted values of F_{ECN}. These rate constants are resolved when the carbachol reaction is monitored by simultaneous hydrolysis of the reporter substrate acetylthiocholine (4,23), and we have inserted predetermined values of k_{21} (which ranged from 0.03 to 0.16 min^{-1}) for each carbachol concentration (4) as a fixed parameter in fitting to eq 6 and A2. Although k_{12} and k_{21} contain important mechanistic information (*e.g.*, (4)), their analysis is not undertaken in this report in order to focus on the useful thermodynamic information obtained by measuring F_{EM} and F_{ECN} over a range of ligand concentrations.

Expressions for k_{12}, k_{21}, *M* and *N* are derived by selecting a particular reaction scheme. One model for the reaction of carbamate substrates with AChE is presented in Scheme 3 (4).

This scheme is simplified from Scheme 1 because k_2 and k_3 with carbamates represent slow reactions that eliminate *E*AP as a significant intermediate and allow all ligand binding to reach equilibrium. The acylated enzyme intermediate *E*A in Scheme 1 becomes the carbamoylated enzyme *E*C in Scheme 3. Since our analysis here assumes no *E*C at time $t = 0$, the relevant species from Scheme 3 and the new species with thioflavin T bound to the P-site at time $t = 0$ are given in Scheme 4.

In Scheme 4 the affinity of thioflavin T (L) at the P-site (denoted by subscript P) is characterized by the dissociation constant K_L in the absence of carbachol (S) and by i_2K_L when S occupies the A-site. When all reactions in Scheme 4 are assumed to reach equilibrium (*e.g.*, $[E][L] = K_L[EL_P]$, etc.), *M* from Scheme 2 is given by eq. 7.

$$M=1+\frac{[S]}{K_{M+S}}+\frac{[L]}{K_L}+\frac{[S]}{K_M}\cdot\left[\frac{[S]}{iK_S}+\frac{[L]}{i_2K_L}\right] \quad (7)$$

In eq 7 K_M is equal to K_SK_1 and K_{M+S} is given in eq. 8.

$$\frac{[S]}{K_{M+S}}=\frac{i[S]}{iK_S}+\frac{[S]}{K_M} \quad (8)$$

Scheme 4 can be linked with Scheme 2 by noting that the only fluorescent complexes in Scheme 4 are $E\mathrm{L_P}$ and $E\mathrm{SL_P}$. The total fluorescence from these complexes is $f_{EL}[E\mathrm{L_P}] + f_{ESL}[E\mathrm{SL_P}]$, where the coefficients f_{EL} and f_{ESL} denote the molar fluorescence of thioflavin T in the binary complex $E\mathrm{L_P}$ and the ternary complex $E\mathrm{SL_P}$, respectively. Therefore, combining this expression with eqs. 4 and 6 leads to eqs 9 and 10.

$$F_0 = F_B + F_{EM}[E]M = F_B + f_{EL}[E\mathrm{L_P}] + f_{ESL}[E\mathrm{SL_P}] \tag{9}$$

$$F_{EM} = \frac{f_{EL}[\mathrm{L}]}{M K_L}\left[1 + \left(\frac{f_{ESL}}{f_{EL}}\right)\left(\frac{[\mathrm{S}]}{i_2 K_M}\right)\right] \tag{10}$$

Eq. 10 is a slightly rewritten form of a previous equation (2), and it assumes that $[\mathrm{L}] \cong [\mathrm{L}]_{tot}$ and $[\mathrm{S}] \cong [\mathrm{S}]_{tot}$. F_{EM} data were initially fitted to eq. 10 by nonlinear regression analysis (SigmaPlot version 10) with [S] as the independent variable, [L], K_L, i and i_2 as fixed parameters, and K_M, iK_S, f_{EL} and f_{EL}/f_{ESL} as the fitted parameters. The value of K_L at the ionic strength employed here was 1.91 μM (23). The only fitted parameter retained from these analyses was f_{EL}, which remained constant at a given [L] over a wide range of the input i and i_2 values. Control reactions with AChE and thioflavin T alone were interspersed with runs that included carbachol to confirm the stability of f_{EL}. A second cycle of data fitting was then conducted in which F_{EM}/f_{EL} from multiple data sets, each at different fixed [L], were analyzed simultaneously with eq 10 in the numerical integration program SCoP (Simulation Resources, Inc., Redlands, CA; version 3.52) as described previously (1). In these simultaneous fits either i or i_2 became one of the four fitted parameters. In addition, K_M was replaced with K_{M+S} as one of the fitted parameters with the substitution $K_M = K_{M+S}iK_S/(iK_S - (i)(K_{M+S}))$ (from eq. 8).

Results and Discussion

The fluorescence of thioflavin T is enhanced by a factor of more than 800 when it binds to AChE (1,23). The fluorescence increase is consistent with thioflavin T interaction at a single site in human AChE with an equilibrium dissociation constant of 1 - 2 μM (23). The structure of the thioflavin T complex with *Tc*AChE obtained by X-ray crystallography (24) indicates that the ligand binds to the AChE P-site, with the benzothiazole ring of thioflavin T stacked against Trp279 and its dimethylaminophenyl moiety 3.5Å distant from and nearly coplanar with the phenyl group of Phe330. The two rings of thioflavin T are planar, and this loss of rotational mobility is thought to provide the fluorescence enhancement in thioflavin T-AChE complexes (see (25). The partial quenching of this fluorescence when an A-site ligand binds to form a ternary complex can also be explained by three-dimensional structures. In crystal structures of *Tc*AChE with two ligands specific for the A-site, edrophonium (26) and TMTFA (11), the phenyl ring of Phe330 is rotated ~115° relative to its position in the thioflavin T-*Tc*AChE complex. In this orientation, the phenyl ring would partially overlap with the crystal structure location of thioflavin T. Therefore, the proximity of the phenyl ring is likely to slightly distort the planarity of thioflavin T and decrease the fluorescence in the ternary complex.

The difference in thioflavin T fluorescence intensity between these binary and ternary complexes allows the binding of both A and P-site ligands to be quantified (1,2). Fluorescence changes when carbachol was rapidly mixed with the binary complex of thioflavin T and AChE depended on the carbachol concentration (Figure 2). With 0.5 mM carbachol in Figure 2, the fluorescence decreased about 25% over the 2-minute time course in which AChE was largely converted to the carbamoylated enzyme EC. At a higher 10 mM concentration of carbachol,

almost no fluorescence change was observed during the reaction, and at 40 and 60 mM carbachol rapid 10 - 15% increases in fluorescence were observed (Figure 2). Thioflavin T can bind to both *E* and *E*C, and the direction of the fluorescence change depended on the relative quenching of complexes formed by *E* and *E*C. The kinetics of the fluorescence change corresponded closely to a single exponential reaction, although a slightly better fit was obtained when a second, minor exponential component was included (Figure 3 and see the Appendix).

To obtain equilibrium binding constants for carbachol with the free enzyme *E*, we focused on the initial fluorescence F_0 prior to the formation of *E*C in reaction traces like those in Figure 2. F_0 (or F_{EM}, which is (F_0 - F_B) normalized by $[E]_{tot}$; see eq 6) decreased progressively with increasing carbachol concentration, consistent with the expected partial quenching of thioflavin T fluorescence in the reversible complex formed when carbachol binds to the A-site in the ternary complex involving *E*. However, analysis of the F_{EM} data is challenging. Scheme 4 includes four independent equilibrium constants for carbachol binding (K_M, K_S, i_2K_M, and iK_S) and two fluorescence coefficients (f_{EL} and f_{ESL}), and it is difficult for an F_{EM} analysis to uniquely assign all six parameters. F_{EM} was obtained as a function of the carbachol concentration from traces like those in Figure 2 in three experiments, each at a different fixed concentration of thioflavin T, and F_{EM}/f_{EL} from these data sets were then fitted simultaneously to eq. 10 as outlined in Figure 4. We previously showed that the equilibrium constants corresponding to K_M and i_2 for the binding of the specific A-site ligand edrophonium in its binary complex with *E* and its ternary complex with *E* and thioflavin T could be assigned unambiguously from a similar combination of fluorescence data sets (1). However, edrophonium does not show significant binding to the P-site (equivalent to eliminating ESS_P in Scheme 4 by setting $iK_S^{-1} = 0$ in eqs 7 and 10). A similar one-site analysis could be applied to the carbachol data (dotted lines in Figure 4), but a better fit was obtained by including iK_S in a two-site analysis. The higher affinity site was occupied by carbachol in the ternary complex with thioflavin T and AChE, and we assume that this is the A-site. The lower affinity site involved competition between carbachol and thioflavin T, and we assume this to be the P-site. The values of some of the fitted parameters, however, had a small dependence on the fixed value of *i* or i_2 (Table 1). The two parameters independent of *i* or i_2 were f_{EL}/f_{ESL} and K_{M+S}, a measure of the combined binding of carbachol to the A- and P-sites (see eq. 8). Ranges for the other fitted parameters are shown in the last two rows of Table 1. These ranges are dictated by the requirements that *i* be positive (fixing i_2 at a maximum of 1.08) and that $iK_S > K_M$ (fixing i_2 at a minimum of 0.42). These are very conservative requirements. Based on previous estimates of i_2 for thioflavin T with edrophonium (1.12, (1) and ATMA (3.1, (2), it is unlikely that either *i* or i_2 with carbachol is much less than 1.0. A reasonable best estimate is to fix i_2 at 0.90, which leads to the fitted parameters in the top row of Table 1 and suggests that the probable range of K_M, iK_S and i_2 is within 20% of their values in this row. Slightly more uncertainty surrounds *i*, as its value is determined by the level of ES_P, a very minor component in these titrations. However, it is likely to lie between 1 and a maximal value of 1.67, obtained when i_2 was fixed at 0.54. Additional studies are required to determine whether even less ambiguity in these values can be achieved with simultaneous fitting of a greater number of data sets at different fixed concentrations of thioflavin T.

One noteworthy comparison arising from Table 1 involves the parameter f_{EL}/f_{ESL}. a measure of the relative quenching of thioflavin T fluorescence in the ternary complex involving free *E*. Its value of 1.50 in Table 1 and was significantly smaller than previous determinations of f_{EL}/f_{ESL} with edrophonium (2.76 ± 0.02, (1) or ATMA (3.0 ± 0.2, (2). We contend above that this relative quenching arises from rotation of the phenyl ring of Phe330 in the ternary complex. The lower value of f_{EL}/f_{ESL} for carbachol therefore implies that carbachol binding to the A-site induces a smaller rotation of the phenyl ring of Phe330 and less distortion of the planarity of thioflavin T in the ternary complex. This explanation is also consistent with the best estimates of 0.9 – 1.0 for *i* and i_2 in Table 1. These values indicate no loss of affinity for the relatively

small carbachol molecule in ternary complexes relative to binary complexes, in contrast to higher i_2 values previously observed for ternary complexes involving larger cationic ligands (3.1 with ATMA and thioflavin T and 9.5 for ATMA and propidium (2). Since carbachol is an isosteric analog of acetylcholine, there is also likely to be little unfavorable steric or electrostatic interaction between bound acetylcholine molecules in AChE ternary complexes.

Information about carbachol binding to the carbamoylated enzyme *E*C is also available from reaction traces like those in Figure 2 through analysis of F_{ECN} (eq 5). While F_{ECN} makes the predominant contribution to the final steady-state fluorescence, F_{ECN} was actually determined by fitting the entire reaction time course to eq A2. Values of F_{ECN}/f_{ECL} in Figure 5 first increased slightly and then decreased with increasing carbachol concentration in each of the three data sets, a biphasic pattern that requires two carbachol binding sites in *E*C. The higher affinity site again involved carbachol binding in the ternary complex, and the most likely candidate is the A-site. There has long been indirect evidence from kinetic analyses that cationic inhibitors can bind to the A-site in acylated AChE even with the site partially occupied by the acyl group (see (5)), and a recent crystallographic study of acetylthiocholine with *Tc*AChE indicated that the P- and A-sites can each be occupied by an acetylthiocholine molecule in the acetylated enzyme (27). Scheme 3 may be extended to allow substrate to bind to the A- and P-sites in the carbamoylated enzyme *E*C as shown in Scheme 5.

One group has in fact attributed one component of substrate inhibition to a block of deacylation when the substrate binds to the A-site in the acylated enzyme ($c = c_2 = 0$ in Scheme 5; (18)), although other interpretations of the kinetic data are possible. In a parallel version of Scheme 4, *E* is replaced by *E*C in all of the proposed enzyme species and the subscripts for all of the kinetic and thermodynamic parameters are prefaced by EC. The resulting expression for F_{ECN} is given in eq 11.

$$F_{ECN} = \frac{f_{ECL}\,[L]}{N\,K_{ECL}}\left[1+\left(\frac{f_{ECSL}}{f_{ECL}}\right)\left(\frac{[S]}{i_{EC2}\,K_{ECM}}\right)\right] \qquad (11)$$

F_{ECN}/f_{ECL} values from data sets at each of the three thioflavin T concentrations were fitted simultaneously to eq. 11 as outlined in Figure 5, and the fitted parameters are shown in Table 2. The format of this table is identical to that in Table 1, and a similar analysis of the range of fitted parameters as that presented for Table 1 above revealed the same pattern of dependence on the fixed values of i_{EC} or i_{EC2}. The overall consistency of the F_{EM} and F_{ECN} data is highlighted by the agreement in the affinities of carbachol for the P-site in *E* (iK_S of 26 mM) and in *E*C ($i_{EC}K_{ECS}$ of 32 mM) and in the small difference in carbachol affinities between binary and ternary complexes (best estimates of i, i_2, i_{EC}, and i_{EC2} are all close to 1). In contrast to the consistent quenching of thioflavin T fluorescence in ternary complexes with carbachol and *E* noted above, the fitted value of f_{ECL}/f_{ECSL} (0.83) indicated that the fluorescence of bound thioflavin T actually increased about 20% when carbachol bound to the A-site in the ternary complex with *E*C. This increase made the determinations of K_{ECM+S} and K_{ECM} possible, but its small magnitude resulted in larger relative errors for these parameters than those for K_{M+S} and K_M in Table 1. Furthermore, the K_{ECM+S} of 1.7 mM was nearly three-fold lower than K_{M+S}, indicating that ECS_P was very minor relative to *E*CS and making estimation of i_{EC} even more difficult than that of i. A very conservative estimate is that i_{EC} is likely to lie between 1 and a maximal value of 5.2, obtained when i_{EC2} was fixed at 0.48.

Calculation of the parameter f_{ECSL}/f_{ESL} (1.14 ± 0.03 for the three sets in Tables 1 and 2, not all data shown) indicates that thioflavin T fluorescence was actually less quenched when carbachol bound to the A-site in the ternary complex with the carbamoylated enzyme $ECSL_P$ than with the free enzyme ESL_P. This suggests less steric interaction between bound

thioflavin T and bound carbachol in ECSL$_P$ than in ESL$_P$. Therefore, if the location of carbachol binding in the A-site is slightly different in E and EC, the somewhat higher affinity of carbachol for the A-site in EC can be rationalized.

An important application of the values determined for the thermodynamic parameters in Tables 1 and 2 is their comparison with independent measurements of some of the same parameters from analyses of k_{12} and k_{21} for carbachol with AChE. These comparisons can be used to support and refine reaction schemes for the AChE catalytic pathway. For example, a preliminary analysis of k_{12} with carbachol did not clearly reveal a second carbachol binding site and thus could not assign values to iK_S, i or i_2, even with the higher precision obtained with acetylthiocholine as the reporter substrate rather than thioflavin T. However, this analysis did estimate K_{M+S} to be 2.8 ± 0.2 mM (4), about 60% of the K_{M+S} value in Table 1. A parallel preliminary analysis of k_{21} assigned a K_{ECM} of 9 ± 1 mM based on the decrease in k_{21} with increasing carbachol concentration (4), a value 5-fold higher than K_{ECM} in Table 2. Despite the uncertainties in the measurement of K_{ECM} here as noted above, this difference appears to be beyond the variance of the measurements and suggests that a revised kinetic model for the previous analysis of k_{21} may be necessary.

Because carbachol is an isosteric analog of acetylcholine and acetylthiocholine, differences in their affinities for the A- and P-sites are likely to reflect their distinctive electronic distributions around the carbonyl carbon atom. The affinities of acetylcholine and acetylthiocholine for the A-site have not been measured, and the likelihood that binding does not reach equilibrium (15,28) will probably prevent their measurement. In contrast to analyses of substrates in equilibrated systems, K_M with these substrates is a combination of rate constants and cannot be used as a measure of affinity. One measurement of acetylthiocholine affinity for the P-site has been made and is based on inhibition of rates of fasciculin association with the P-site. The reported value of about 1 mM (15) was obtained at a somewhat lower ionic strength than employed here, but even compensating conservatively for this difference the 26 and 32 mM values of iK_S and $i_{EC}K_{ECS}$ for the binding of carbachol to the P-site in Tables 1 and 2 are an order of magnitude higher than that expected for iK_S with acetylthiocholine. Acetylthiocholine appears to interact with W286, F337, Y124, Y72 (27,29) and indirectly with D74 (17) in the P-site, and further studies are necessary to determine the precise interactions that increase its affinity by an order of magnitude over carbachol in this site.

Appendix

Carbamate reactions with AChE are fitted fairly well with the single exponential formulation in Scheme 2 and eqs 1 and 2, but slightly better fits are obtained if a minor second exponential term is added (T. L. Rosenberry *et al.*, manuscript in preparation). We assumed that the second minor exponential corresponded to carbachol reactions with a small amount of AChE (E2) with slightly different catalytic properties from those of the major AChE component E1. A similar small component was observed previously during measurements of organophosphate reactions with our recombinant human AChE, and we attributed it to a minor AChE form (16), perhaps differing in the size or location of glycosyl groups. The corresponding extension of eq 5 is given in eq A1, where 2 denotes terms involving the minor E2 component.

$$F=F_B+F_{EM}[E]M+F_{ECN}[EC]N+F_{EM2}[E2]M2+F_{ECN2}[EC2]N2 \quad (A1)$$

The E2 component was only slightly evident with the carbachol reactions monitored by thioflavin T fluorescence here (see Figure 3), but it was much clearer with the fluorogenic carbamate M7C and with carbachol reactions monitored with acetylthiocholine as a reporter

substrate (4), where values of $R = [E2]_{tot}/[E1]_{tot}$ of 0.02 to 0.10 were obtained (T. L. Rosenberry *et al.*, manuscript in preparation). Here, R was fixed at 0.05. The intent in including *E*2 in analyzing carbamate reactions was simply to improve the accuracy of values assigned to the major component *E*1, and no analysis of reactions involving *E*2 was attempted. The precision of our measurements was sufficient to indicate only that the corresponding k_{122} for *E*2 was 3- to 10-fold lower than the k_{12} for *E*1. In the absence of evidence of other differences between the major and minor reaction components, k_{21}, F_{EM}, and F_{ECN} were assumed to be the same for both components. Eq 6 then is extended to eq A2.

$$F=F_B+F_{EM}[E]_{tot}+\frac{(F_{ECN}-F_{EM})[E]_{tot}\,k_{12}}{(1+R)(k_{12}+k_{21})}\left(1-e^{-[(k_{12}+k_{21})\,t]}\right)+\frac{R(F_{ECN}-F_{EM})[E]_{tot}\,k_{122}}{(1+R)(k_{122}+k_{21})}\left(1-e^{-[(k_{122}+k_{21})\,t]}\right) \quad \text{eq. (A2)}$$

References

1. De Ferrari GV, Mallender WD, Inestrosa NC, Rosenberry TL. Thioflavin T is a fluorescent probe of the acetylcholinesterase peripheral site that reveals conformational interactions between the peripheral and acylation sites. J. Biol. Chem 2001;276:23282–23287. [PubMed: 11313335]
2. Johnson JL, Cusack B, Davies MP, Fauq A, Rosenberry TL. Unmasking tandem site interaction in human acetylcholinesterase. Substrate activation with a cationic acetanilide substrate. Biochemistry 2003;42:5438–5452. [PubMed: 12731886]
3. Brufani M, Lippa S, Marta M, Oradei A, Pomponi M. Acetylcholinesterase inhibition by eserine: rate constants of reaction. Part II. Ital. J. Biochem 1985;34:328–340. [PubMed: 4077467]
4. Rosenberry TL, Johnson JL, Cusack B, Thomas J, Emani S, Venkatasubban KS. Interactions between the peripheral site and the acylation site in acetylcholinesterase. Chem. Biol. Interact 2005;157-158:181–189. [PubMed: 16256966]
5. Rosenberry, TL. Acetylcholinesterase. In: Meister, A., editor. Advances in Enzymology. John Wiley & Sons; New York: 1975. p. 103-218.
6. Giacobini, E. Cholinesterase inhibitors: from the Calabar bean to Alzheimer therapy. In: Giacobini, E., editor. Cholinesterases and Cholinesterase Inhibitors. Martin Dunitz; London: 2000. p. 181-226.
7. Rosenberry TL. Quantitative simulation of endplate currents at neuro-muscular junctions based on the reactions of acetylcholine with acetylcholine receptor and acetylcholinesterase. Biophys. J 1979;26:263–290. [PubMed: 262418]
8. Changeux J-P. Responses of acetylcholinesterase from *Torpedo marmorata* to salts and curarizing drugs. Mol. Pharmacol 1966;2:369–392. [PubMed: 5970686]
9. Taylor P, Lappi S. Interaction of fluorescence probes with acetylcholinesterase. The site and specificity of propidium binding. Biochemistry 1975;14:1989–1997. [PubMed: 1125207]
10. Sussman JL, Harel M, Frolow F, Oefner C, Goldman A, Toker L, Silman I. Atomic structure of acetylcholinesterase from *Torpedo californica*: A prototypic acetylcholine-binding protein. Science 1991;253:872–879. [PubMed: 1678899]
11. Harel M, Quinn DM, Nair HK, Silman I, Sussman JL. The X-ray structure of a transition state analog complex reveals the molecular origins of the catalytic power and substrate specificity of acetylcholinesterase. J. Am. Chem. Soc 1996;118:2340–2346.
12. Harel M, Kleywegt GJ, Ravelli RBG, Silman I, Sussman JL. Crystal structure of an acetylcholinesterase-fasciculin complex: interaction of a three-fingered toxin from snake venom with its target. Structure 1995;3:1355–1366. [PubMed: 8747462]
13. Bourne Y, Taylor P, Marchot P. Acetylcholinesterase inhibition by fasciculin: Crystal structure of the complex. Cell 1995;83:503–512. [PubMed: 8521480]
14. Szegletes T, Mallender WD, Rosenberry TL. Nonequilibrium analysis alters the mechanistic interpretation of inhibition of acetylcholinesterase by peripheral site ligands. Biochemistry 1998;37:4206–4216. [PubMed: 9521743]

15. Szegletes T, Mallender WD, Thomas PJ, Rosenberry TL. Substrate binding to the peripheral site of acetylcholinesterase initiates enzymatic catalysis. Substrate inhibition arises as a secondary effect. Biochemistry 1999;38:122–133. [PubMed: 9890890]

16. Mallender WD, Szegletes T, Rosenberry TL. Organophosphorylation of acetylcholinesterase in the presence of peripheral site ligands: Distinct effects of propidium and fasciculin. J. Biol. Chem 1999;274:8491–8499. [PubMed: 10085081]

17. Mallender WD, Szegletes T, Rosenberry TL. Acetylthiocholine binds to Asp74 at the peripheral site of human acetylcholinesterase as the first step in the catalytic pathway. Biochemistry 2000;39:7753–7763. [PubMed: 10869180]

18. Stojan J, Brochier L, Alies C, Colletier JP, Fournier D. Inhibition of *Drosophila melanogaster* acetylcholinesterase by high concentrations of substrate. Eur. J. Biochem 2004;271:1364–1371. [PubMed: 15030487]

19. Stojan J, Golicnik M, Fournier D. Rational polynomial equation as an unbiased approach for the kinetic studies of *Drosophila melanogaster* acetylcholinesterase reaction mechanism. Biochim. Biophys. Acta 2004;1703:53–61. [PubMed: 15588702]

20. Lakowicz, JR. Principles of Fluorescence Spectroscopy. Vol. 2nd ed.. Kluwer Academic/Plenum; New York: 1999.

21. Rosenberry TL, Bernhard SA. Studies of catalysis by acetylcholinesterase: Fluorescent titration with a carbamoylating agent. Biochemistry 1971;10:4114–4120. [PubMed: 5168614]

22. Rosenberry TL, Bernhard SA. Studies on catalysis by acetylcholinesterase: Synergistic effects of inhibitors during hydrolysis of acetic acid esters. Biochemistry 1972;11:4308–4321. [PubMed: 5079901]

23. Rosenberry TL, Sonoda LK, Dekat SE, Cusack B, Johnson JL. Monitoring the reaction of carbachol with acetylcholinesterase by thioflavin T fluorescence and acetylthiocholine hydrolysis. Chem.-Biol. Interact. 2008in press

24. Harel M, Sonoda LK, Silman I, Sussman JL, Rosenberry TL. The crystal structure of thioflavin T bound to the peripheral site of *Torpedo californica* acetylcholinesterase reveals how thioflavin T acts as a sensitive fluorescent reporter of ligand binding to the acylation site. J. Am. Chem. Soc. 2008in press

25. Friedhoff P, Schneider A, Mandelkow EM, Mandelkow E. Rapid assembly of Alzheimer-like paired helical filaments from microtubule-associated protein tau monitored by fluorescence in solution. Biochemistry 1998;37:10223–10230. [PubMed: 9665729]

26. Harel M, Schalk I, Ehret-Sabatier L, Bouet F, Goeldner M, Hirth C, Axelsen PH, Silman I, Sussman JL. Quaternary ligand binding to aromatic residues in the active-site gorge of acetylcholinesterase. Proc. Natl. Acad. Sci. USA 1993;90:9031–9035. [PubMed: 8415649]

27. Colletier JP, Fournier D, Greenblatt HM, Stojan J, Sussman JL, Zaccai G, Silman I, Weik M. Structural insights into substrate traffic and inhibition in acetylcholinesterase. EMBO J 2006;25:2746–2756. [PubMed: 16763558]

28. Rosenberry TL. Catalysis by acetylcholinesterase. Evidence that the rate-limiting step for acylation with certain substrates precedes general acid-base catalysis. Proc. Nat. Acad. Sci. USA 1975;72:3834–3838. [PubMed: 668]

29. Bourne Y, Radic Z, Sulzenbacher G, Kim E, Taylor P, Marchot P. Substrate and product trafficking through the active center gorge of acetylcholinesterase analyzed by crystallography and equilibrium binding. J. Biol. Chem 2006;281:29256–29267. [PubMed: 16837465]

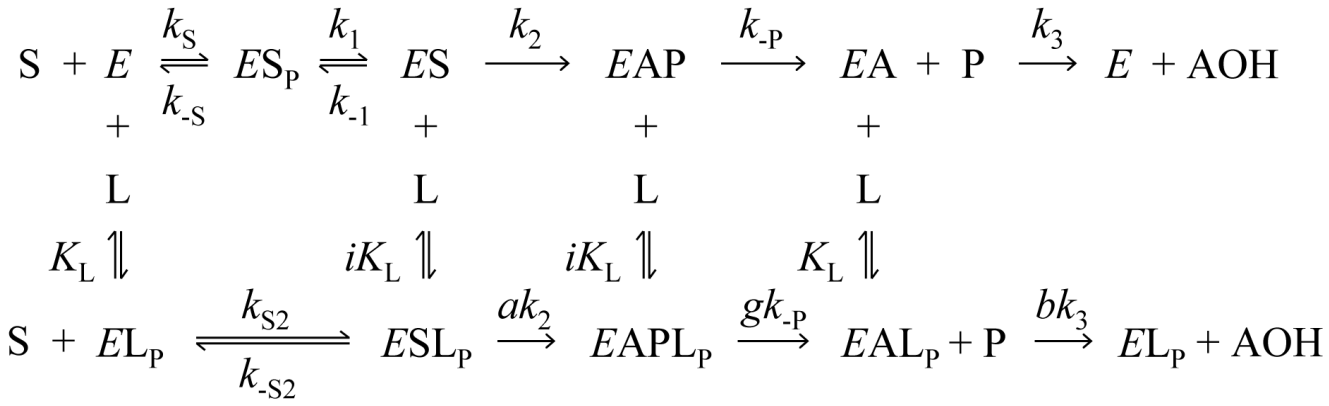

SCHEME 1.

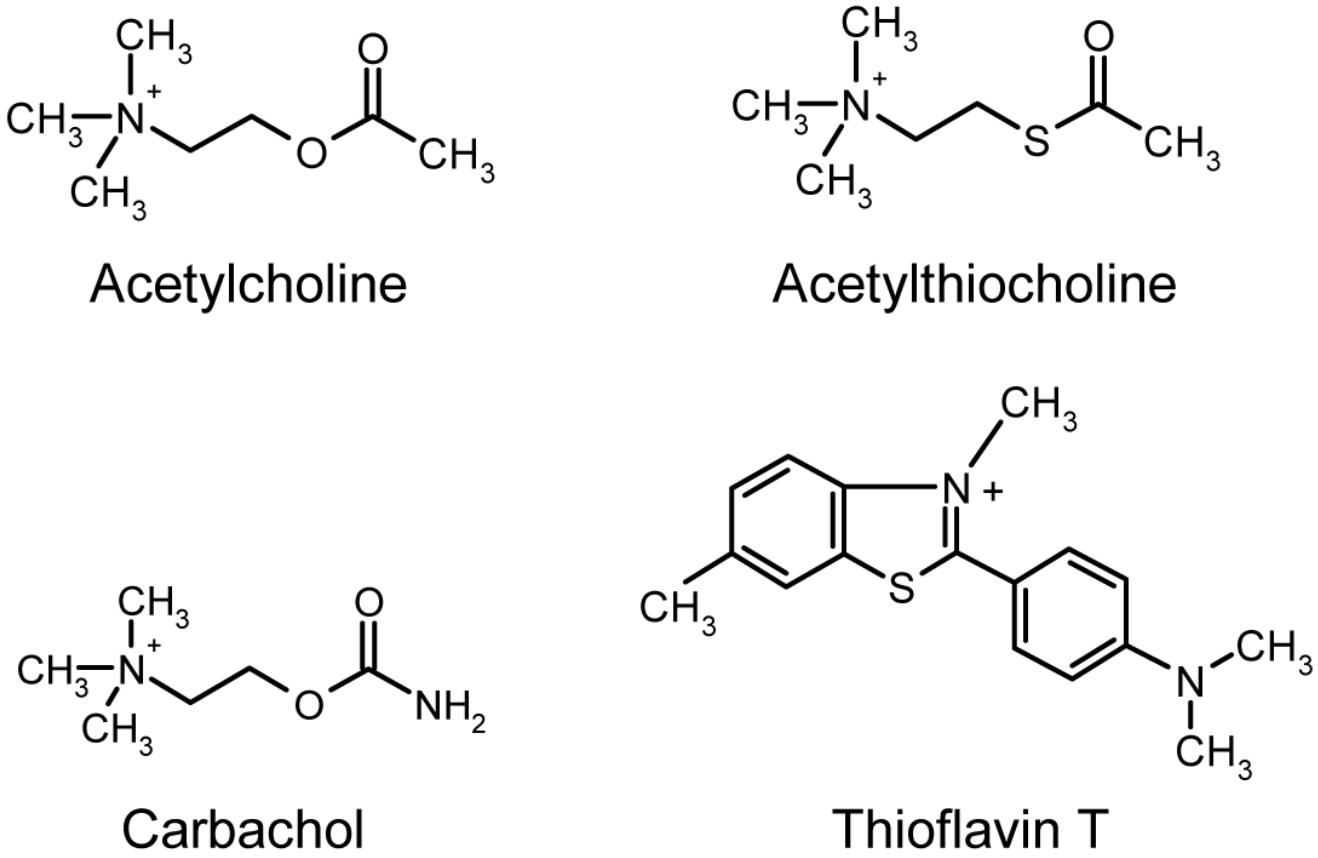

Figure 1.
Structures of acetylcholine analogs and thioflavin T.

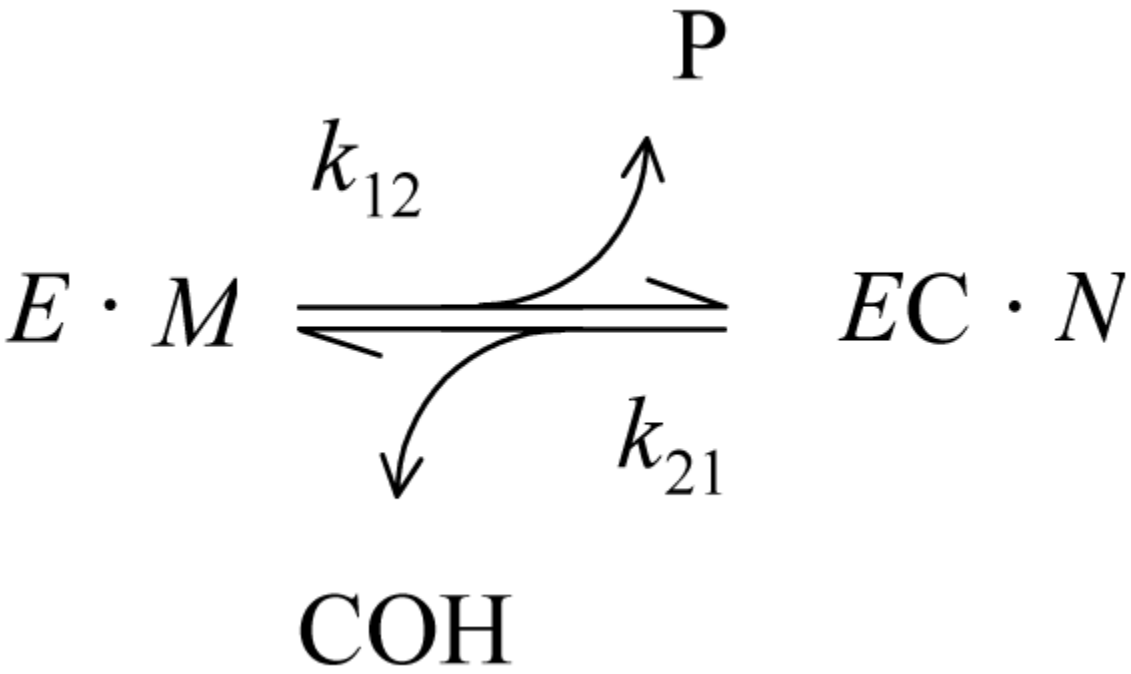

SCHEME 2.

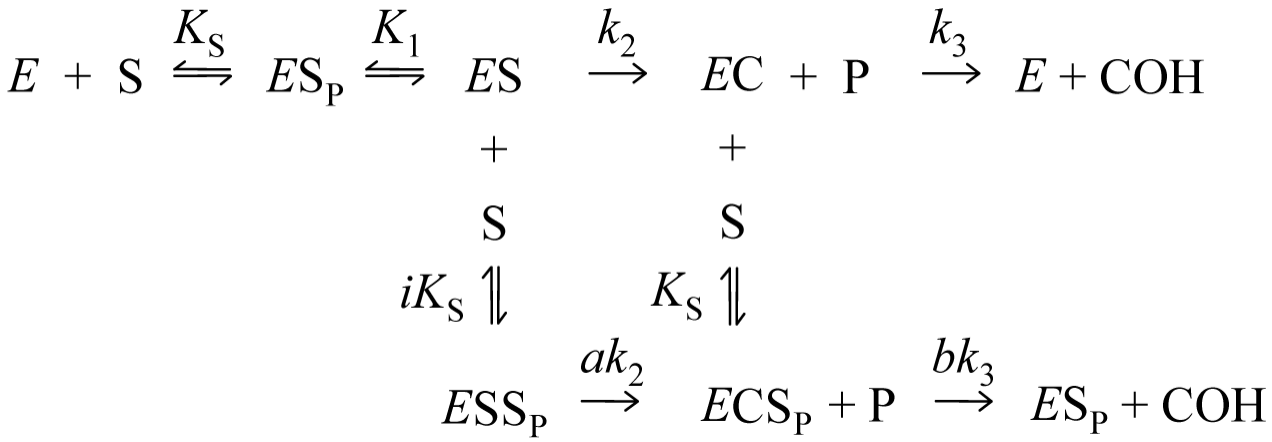

SCHEME 3.

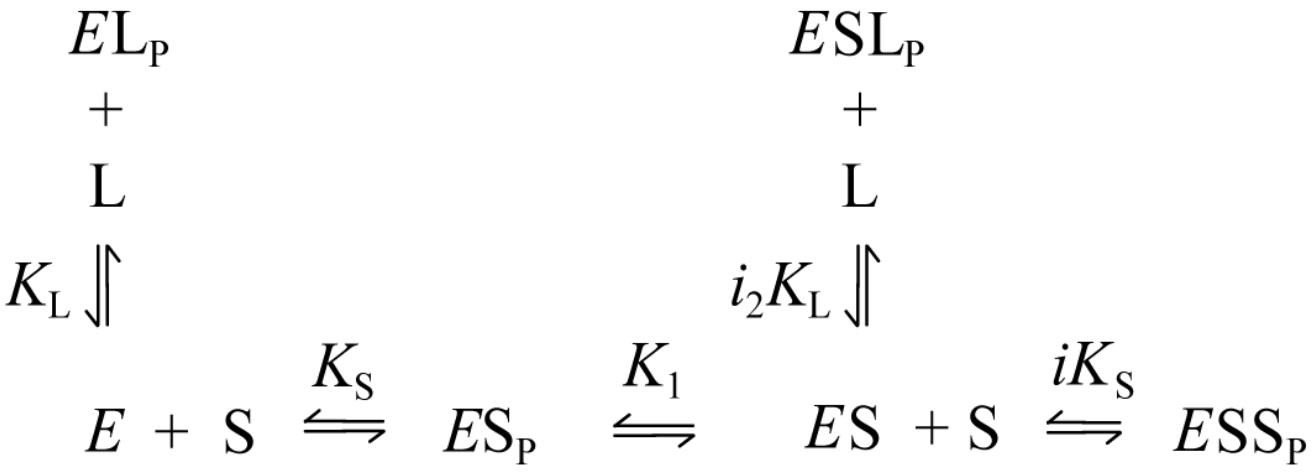

SCHEME 4.

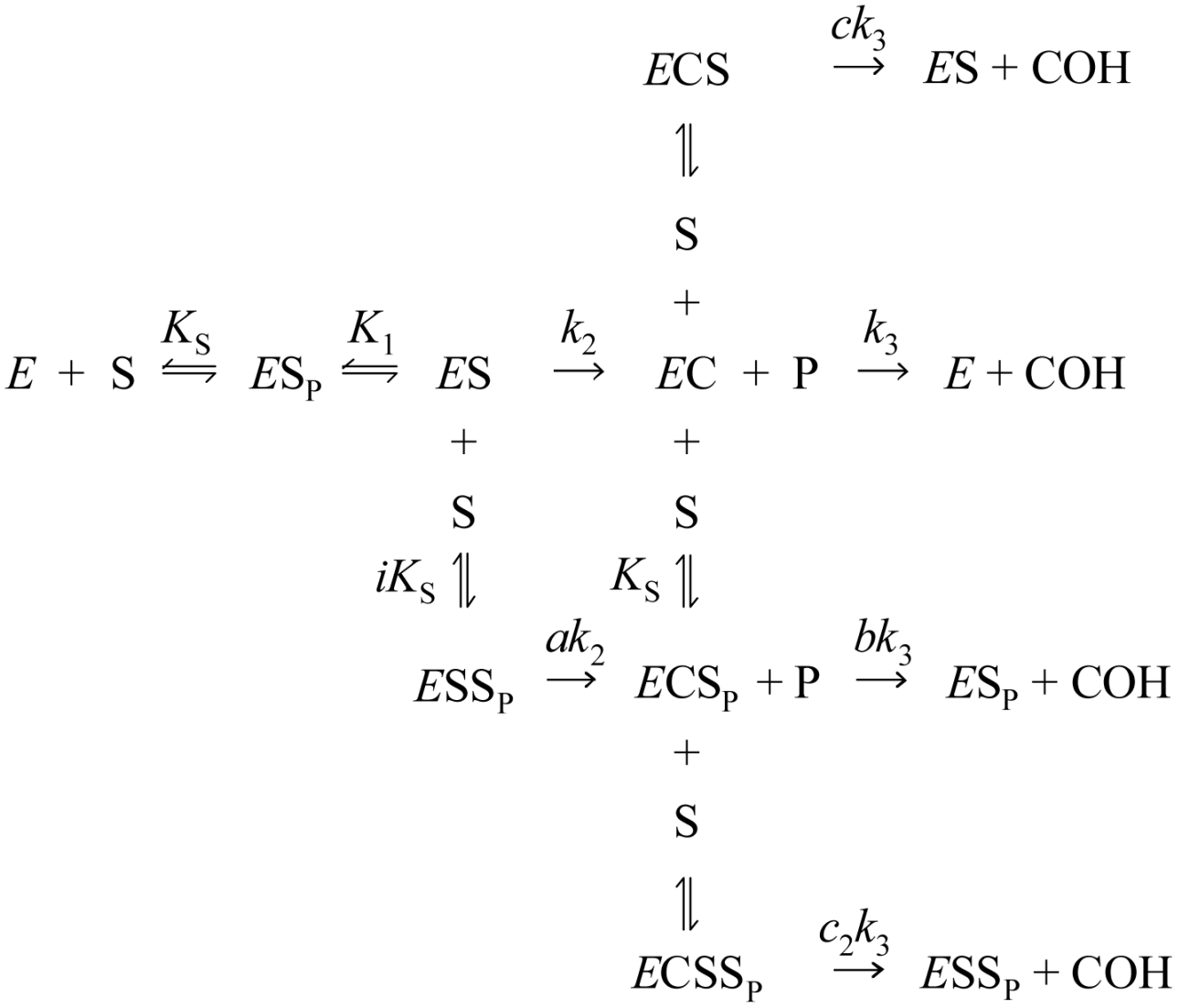

SCHEME 5.

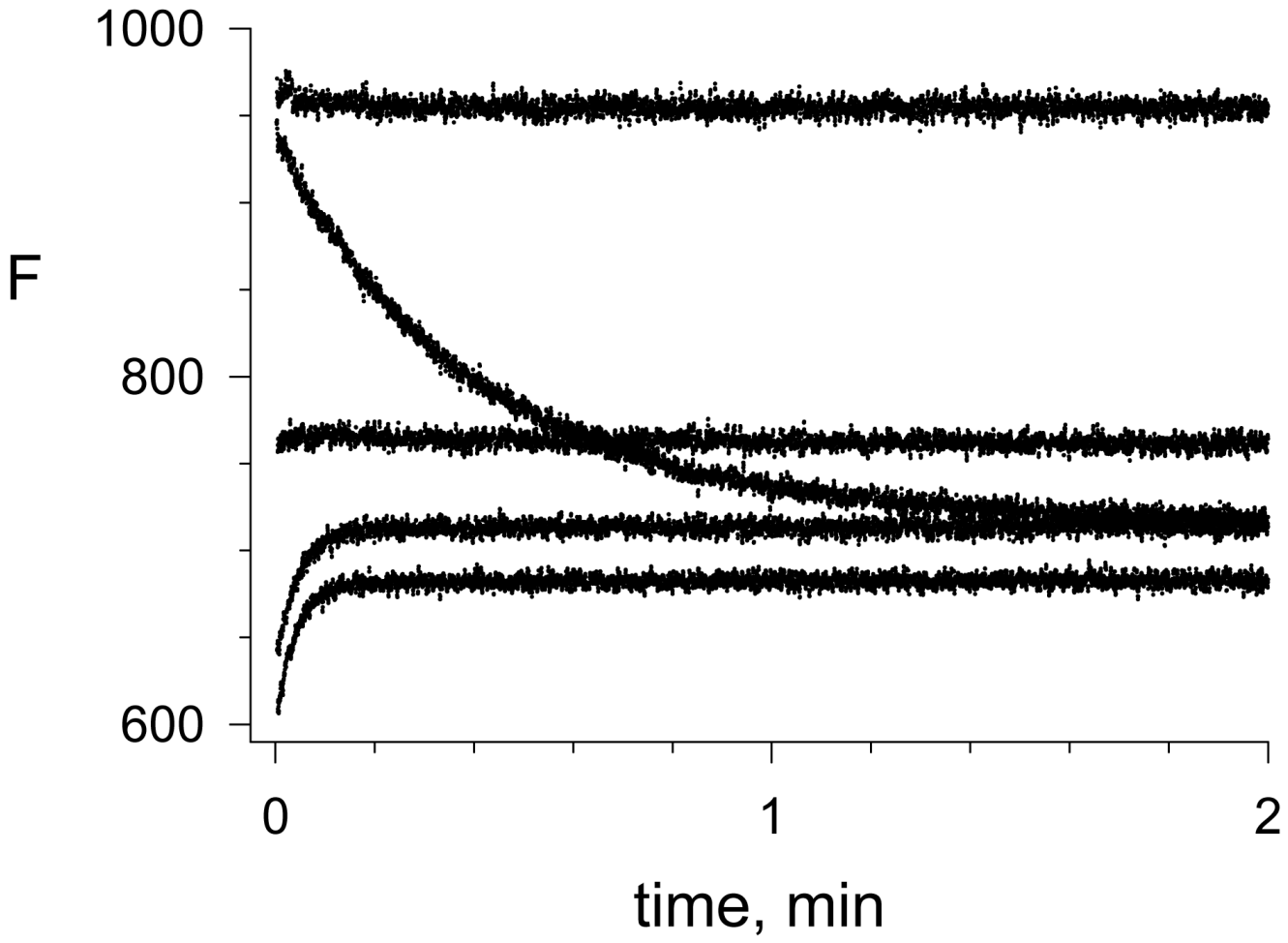

Figure 2.
Reactions of carbachol with AChE monitored by thioflavin T fluorescence. Reactions were initiated by stopped-flow mixing of AChE with carbachol and thioflavin T as outlined in the Experimental Procedures, and the fluorescence F was recorded continuously. Initial concentrations of thioflavin T (15.6 μM) and AChE (152 nM) were the same in each reaction, while the respective concentrations of carbachol were 0, 0.5, 10, 40, and 60 mM (from the upper to the lower trace taken at time $t = 0$). F_B (eq 5) from the components individually was 83.

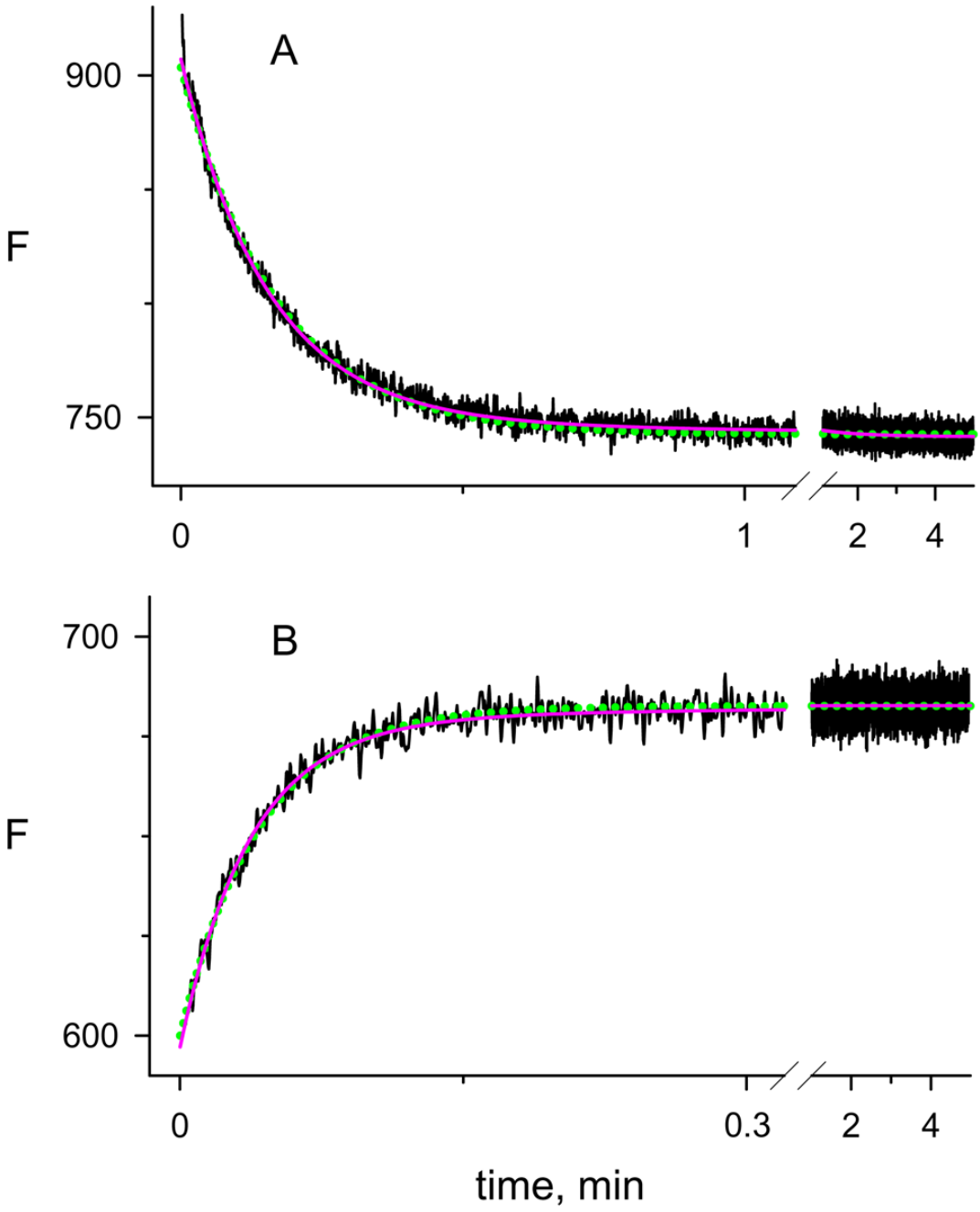

Figure 3.

Analysis of a reaction of carbachol with AChE. Reaction traces were obtained in the presence of thioflavin T under the conditions in Figure 2 with 1.67 mM carbachol in Panel A or 60 mM carbachol in Panel B. Traces were analyzed in SigmaPlot both with the one-component, single-exponential fit in eq 6 and the two-component, double exponential fit in eq A2 in the Appendix to obtain values of F_{EM}, F_{ECN}, and $k_{12} + k_{21}$. The solid red line shows the two-component fit and the dotted green line indicates the one-component fit. Respective values of $k_{12} + k_{21}$ for the overall one- and two-component fits were 5.94 ± 0.02 and 6.53 ± 0.02 min^{-1} in Panel A and 23.8 ± 0.3 and 27.0 ± 0.4 min^{-1} in Panel B. In the two-component fits, k_{122} = 0.68 ± 0.04 in Panel A and 4.3 ± 0.3 in Panel B.

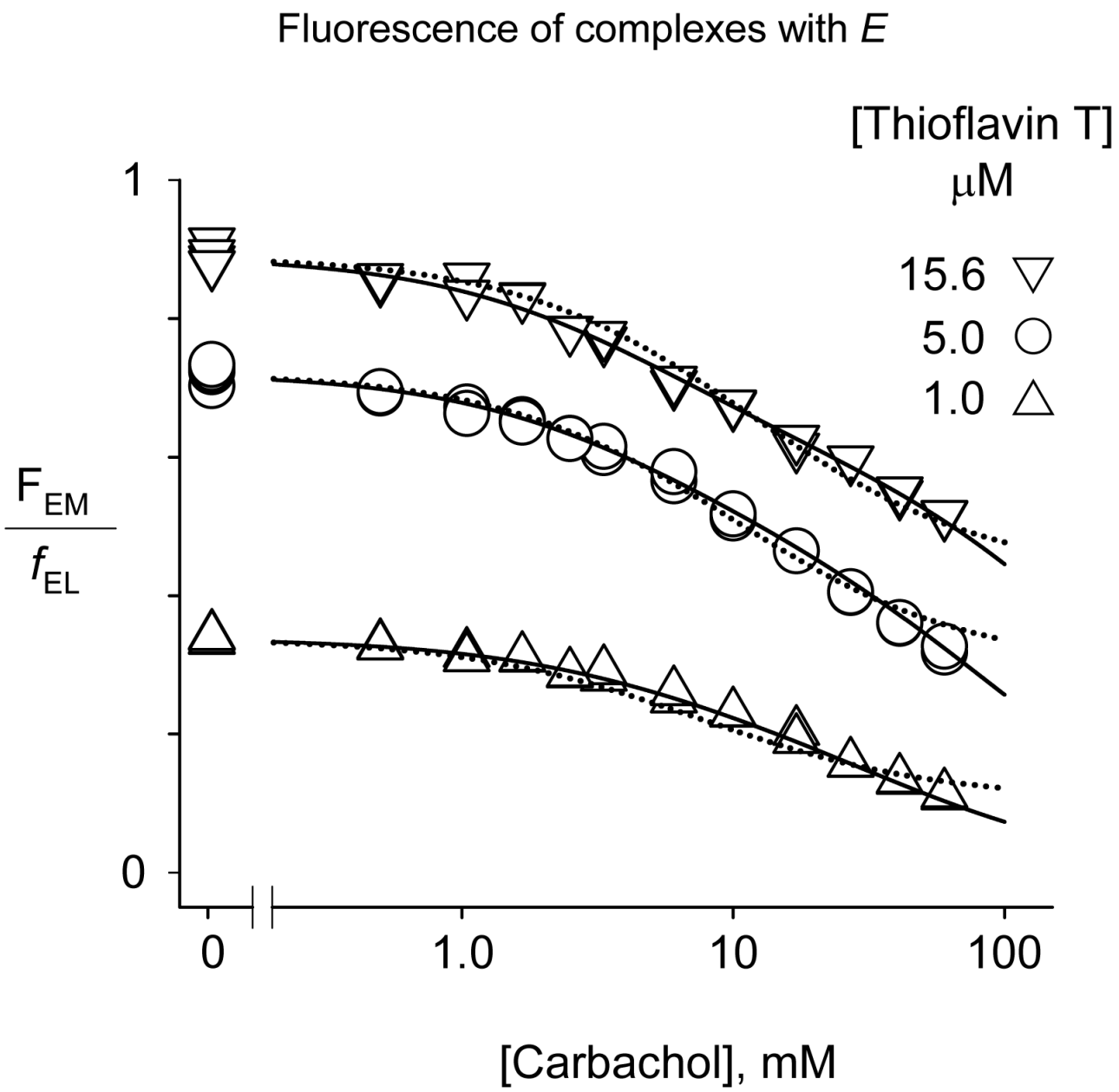

Figure 4.

Determination of carbachol binding constants with free AChE from the initial fluorescence of AChE-bound thioflavin T. From reference (23). F_{EM} values from mixtures of AChE (70 - 155 nM), thioflavin T (1.0 - 15.6 μM, as noted), and the indicated concentration of carbachol were determined from stopped-flow traces as in Figure 3. The F_{EM} data from each set at fixed thioflavin T concentration were fitted initially to eq 10 to obtain f_{EL} for the set, and F_{EM}/f_{EL} from all three sets were then analyzed simultaneously with eq 10 as described in the Experimental Methods. Parameters obtained from the data fitting are shown in Table 1. The dotted lines show the one-site fit when carbachol is assumed to have no affinity for the P-site ($(iK_S)^{-1}$ fixed at 0) with fitted parameters K_{M+S} = 6.2, f_{EL}/f_{ESL} = 1.85, and i_2 =2.1.

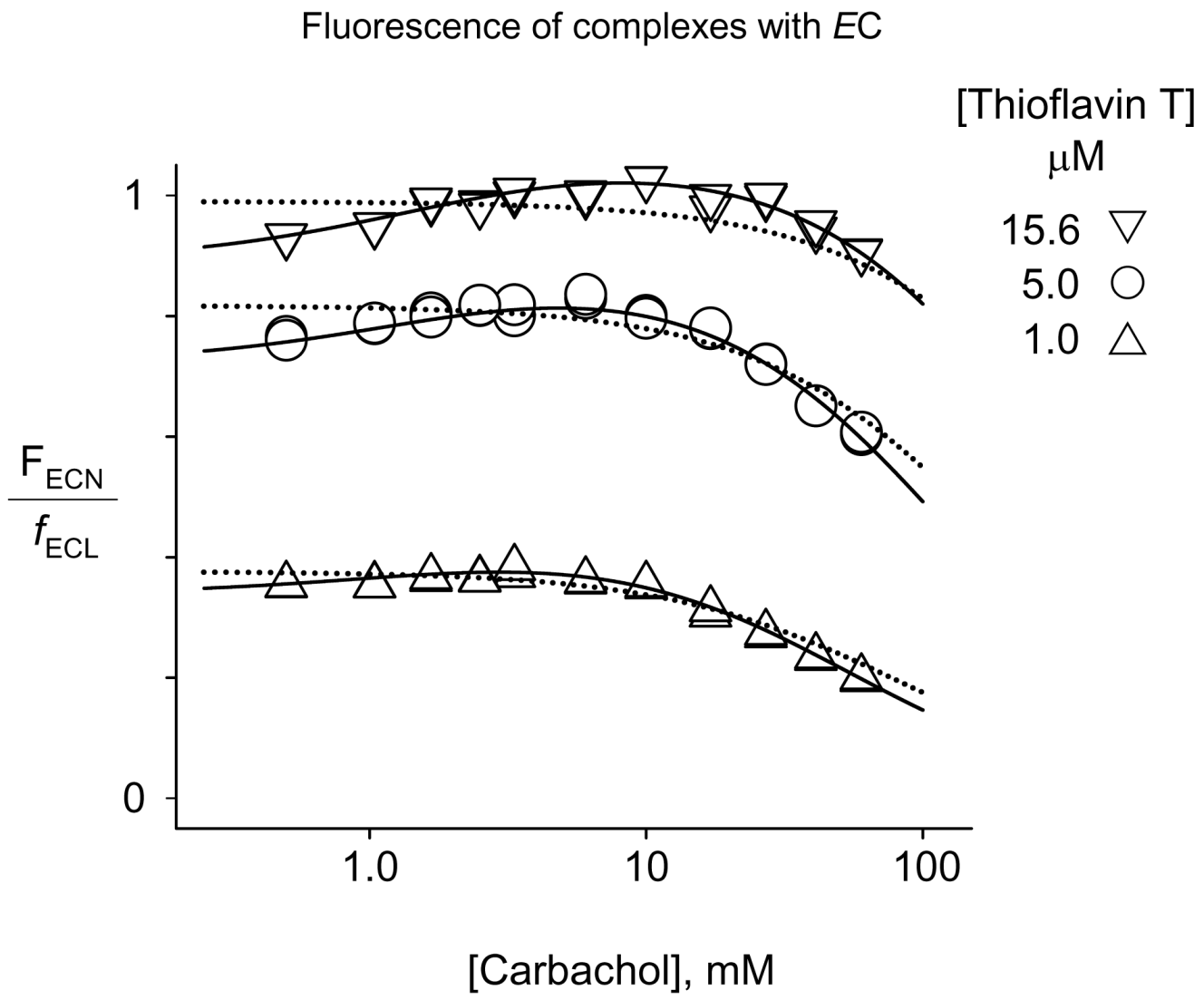

Figure 5.

Determination of carbachol binding constants with carbamoylated AChE from the fluorescence of AChE-bound thioflavin T after the carbachol reactions have reached a final steady state. F_{ECN} values from mixtures of AChE (70 - 155 nM), thioflavin T (1.0 - 15.6 μM, as noted), and the indicated concentration of carbachol were determined from stopped-flow traces as in Figure 3. The F_{ECN} and then F_{ECN}/f_{ECL} data were analyzed with eq 11 as described for F_{EM} and then F_{EM}/f_{EL} in Figure 4. Parameters obtained from the data fitting are shown in Table 2. The dotted lines show the fit when carbachol is assumed to bind to only one site, (*e.g.*, carbachol and thioflavin T compete for the P-site: $(i_{EC}K_{ECS})^{-1}$ and i_{EC2}^{-1} fixed at 0 with fitted K_{M+S} = 57).

Table 1

Thermodynamic constants for carbachol binding to free AChE (*E*) from the thioflavin T fluorescence coefficients F_{EM}/f_{EL}.

	i_2	i	K_{M+S} mM	K_M mM	iK_s mM	f_{EL}/f_{ESL}
a	0.90 fixed	0.92	4.7 ± 0.4	5.7 ± 0.4	26 ± 4	1.50 ± 0.04
b	1.08	1e-6 fixed	4.72	4.72	32	1.50
b	0.42	1.59	4.72	12	12 fixed	1.50

From reference (23). K_L was fixed at 1.91 μM in all analyses. K_M was calculated from eq. 8.

[a] Parameters from the simultaneous fit of the three data sets in Figure 4. Errors (SEM) were obtained by reanalyzing each data set individually with *i* fixed at 0.92, i_2 fixed at 0.90, and K_{M+S}, iK_S, f_{EL} and f_{EL}/f_{ESL} as the fitted parameters. Fitted parameter values from the three individual sets were then averaged and SEM was determined.

[b] Simultaneous fits of the three data sets in Figure 5 with fixed values selected to show maximum parameter range (see text).

Table 2

Thermodynamic constants for carbachol binding to carbamoylated AChE (*E*C) from the thioflavin T fluorescence coefficients F_{ECN}/f_{ECL}.

	***i*EC2**	***i*EC**	***K*ECM+S mM**	***K*ECM mM**	***i*EC*K*ECS mM**	***f*ECL/*f*ECSL**
a	0.90 fixed	1.23	1.7 ± 0.4	1.8 ± 0.5	32 ± 2	0.83 ± 0.01
b	0.96	1e-6 fixed	1.66	1.66	34	0.83
b	0.21	3.5	1.66	8	8 fixed	0.83

Analyses of F_{ECN} were conducted with eq 11 and the data in Figure 5 following the fitting procedures described for F_{EM} in footnotes *a* and *b* in Table 1. One measurement of K_{ECL} = 1.82 ± 0.26 μM in the presence of 2 mM carbachol agreed with the previously determined K_L (1.91 ± 0.18 μM from four experiments; (23)), and K_{ECL} was also fixed at 1.91 μM in all analyses. Thermodynamic parameters correspond to a modified Scheme 4 in which *E* is replaced by *E*C and all subscripts are preceded by EC. Errors (SEM) were obtained by reanalyzing each data set individually with i_{EC} fixed at 1.23 and i_{EC2} fixed at 0.90.